Focused on Crack Tip Fields

Visual Abstract

The ab-initio aided strain gradient elasticity theory: a new concept for fracture nanomechanics

Tomáš Profant, Jaroslav Pokluda

Brno University of Technology, Technická 2896/2, 616 69 Brno, Czech Republic
profant@fme.vutbr.cz, pokluda@fme.vutbr.cz

ABSTRACT. When the width of cracked nanocomponents made of brittle or quasi-brittle materials is less than approximately $10\,\mathrm{nm}$, the size of the K-dominance zone becomes smaller than $2-3\,\mathrm{nm}$ and comparable to the fracture process zone $(0.4-0.6\,\mathrm{nm})$. The fracture process starts to be dominated by far-stress field terms and the critical stress intensity factor can no more represent the total fracture driving force. This means a breakdown of a classical linear elastic fracture mechanics suffering from the undesirable crack-tip stress singularity. The contribution presents a new concept expected to properly predict the critical crack driving force for nano-components: The ab-initio aided strain gradient elasticity theory (AI-SGET). In contrast to the Barenblatt cohesive model, the strain gradient elasticity theory does not require to prescribe a suitable field of cohesive tractions along the crack faces in order to eliminate the stress singularity and to exhibit cusp-like profiles of crack flanks close to the crack front in accordance with atomistic models. The only unknown and necessary quantity is the material length scale parameter which can be, e.g., determined by best strain gradient elasticity fits of ab-initio computed phonon-dispersions and near-dislocation displacement fields. Atomistic approaches can also be employed to determine fracture mechanical parameters (crack driving force, crack tip opening displacement) related to the moment of crack instability in a given material. Such AI-SGET codes can then be utilized to a successful prediction of fracture of cracked nanocomponents made of brittle or quasi-brittle materials.

KEYWORDS. Strain gradient elasticity; Ab-initio adjustment; Stress singularity; Cusp-like crack profile; Cracked nanopanel.

OPEN ACCESS

Citation: Profant, T., Pokluda., J., The ab-initio aided strain gradient elasticity theory: a new concept for fracture nanomechanics, Frattura ed Integrità Strutturale, 49 (2019) 107-114.

Received: 30.04.2019
Accepted: 25.05.2019
Published: 01.07.2019

INTRODUCTION

The basic hypothesis of linear fracture mechanics says that the size of the K-dominant region must be much higher than the fracture process zone incorporating inelastic deformations near the crack-tip. This gives rise to a question regarding the sufficiency of the stress intensity factor to predict the fracture toughness of nano-structures. Shimada et al. in [1] indeed showed that beyond a certain critical size of a nano-component (the specimen

width below approximately $10-15\,\mathrm{nm}$), the classical continuum approach breaks down and the K - dominance zone smaller than $2-3\,\mathrm{nm}$ becomes comparable to the fracture process zone of a constant size of about 0.5 nm where, according to atomistic models, a highly localized discrete motion of atoms takes place. The fracture process then starts to be dominated by far-stress field terms, the stress intensity factor becomes size dependent and can no more be used for characterizing the fracture toughness of cracked nano-structures. Similar behavior also exhibits the Griffith energy release rate (ERR). There are attempts in literature to capture the size dependency of the critical stress intensity factor K_c using a two parameter model based on Williams's expansion but the size dependency of both K_c and the critical ERR contradicts the constant critical ERR obtained from atomistic simulations [2]. It was proved in [3] that Mindlin's strain gradient elasticity theory (SGET, [4]) allows the continuum assumption to be extended beyond the limit of the classical fracture mechanics. In contrast to the Barenblatt cohesive model, the strain gradient elasticity theory does not require to prescribe a suitable field of cohesive tractions along the crack faces in order to eliminate the undesirable stress singularity and to produce cusp-like profiles of near-tip crack faces in accordance with atomistic models even when the simplest form of the SGET is used containing elastic constants and one length material parameter only. The crucial point is to identify this internal length scale parameter. This length parameter can be determined by fitting the ab initio solutions for (i) the displacement field near a screw dislocation, (ii) the critical crack tip opening displacement and (iii) the phonon dispersions using a finite element code based on the SGET. It is worth to note that all the three methods should give equivalent results. Atomistic approaches can also be employed to determine fracture mechanical parameters (crack driving force, crack tip opening displacement) related to the moment of crack instability in a given material. Coupling of these calibration procedures with the SGET-based finite element (FE) code then leads to a multi-scale approach we call *the ab-initio aided strain gradient elasticity theory (AI-SGET)*.

This article is focused on a comparison of Barenblatt and SGET solutions of the stress-strain crack tip field to demonstrate a usefulness of the AI-SGET as well as its capability to remove the stress singularity and to exhibit the near-tip cusp-like profile of crack flanks.

CLASSICAL VS. STRAIN GRADIENT ELASTICITY SOLUTION

The classical elasticity is not able to describe the process region at the crack tip by simply applying the equilibrium and boundary conditions prevailing at the crack front. A special model has to be used to describe the mechanical behavior inside the process region. Probably the most popular known is the Barenblatt model, see Fig. 1a. It is assumed that the Barenblatt region is developed in an isotropic elastic surrounding to be subjected to the classical linear elasticity laws. If the cohesive stress density $\sigma'_{yy}(x)$ is given, then the displacements in the process region in the range $0<x<r_p$ for semi-infinite solid $y\geq 0$ are evaluated as the superposition of displacements ahead and behind the crack tip, respectively,

$$(1-k^2)\mu u_y^+(r_p-\varepsilon r_p)\approx -\frac{2}{3\pi}\int_0^1 \frac{\sigma'_{yy}(r_p-\alpha r_p)}{\sqrt{\alpha}}\varepsilon^{3/2} r_p \mathrm{d}\alpha \qquad \text{for } \varepsilon=\frac{r_p-x}{r_p}\ll 1. \tag{1}$$

The detailed derivation of (1) can be found in [5]. The exponent of the non-dimensional coordinate $\varepsilon^{3/2}$ in (1) provides a smooth cusp-like opening of the crack face. Although the stress density σ'_{yy} is unknown, from the condition

$$\int_0^1 \frac{\sigma'_{yy}(r_p-\alpha r_p)}{\sqrt{\alpha}}\mathrm{d}\alpha<0 \tag{2}$$

follows a decreasing character of the cohesion-decohesion curve as depicted in Fig. 1 in terms of stress density σ'_{yy} and displacement of the upper crack face u_y^+. The Barenblatt model confirms the fact that the classical theories can be applicable in a multi-scale range and even in the nano-scale regime. Although the smooth opening of the crack tip is estimated in (1), the stress conditions prevailing at the crack tip can be evaluated only when the cohesion-decohesion

relations are known. These relations are hidden in the unknown stress density σ'_{yy} and their creation is the topic of many works, e.g. [6, 7].

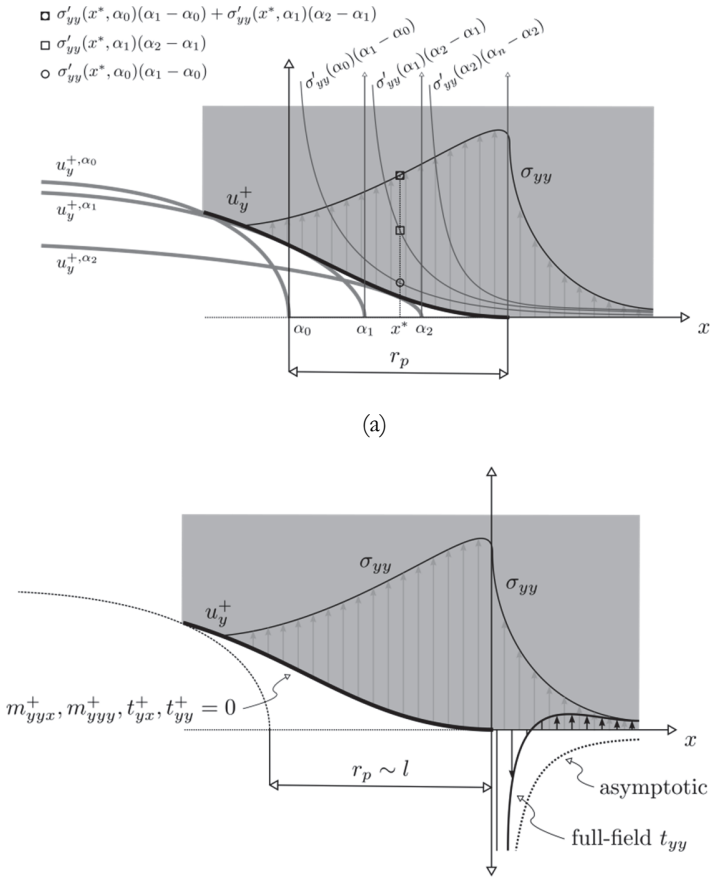

Figure 1: The comparison of the (a) Barenblatt model of the process zone and (b) the process zone in SGET. The cohesion-decohesion stress at the point x^* as the superposition of the monopolar stress differentials $\sigma'_{yy}\mathrm{d}\alpha$ is symbolically depicted in the Barenblatt model (a). The boundary condition of the stress free crack faces as well as the asymptotic and full-filed total stresses t_{yy} ahead of the crack tip are visualised in the SGET model (b).

A second way how to avoid the break-down of the classical fracture mechanics at the nanoscale is an application of the SGET model introduced by Mindlin. A detailed presentation of the Form II of the Mindlin's theory can be found in [8-11]. Here the strain energy density $W = W(\varepsilon_{ij}, \partial_k \varepsilon_{ij})$ is a function of the linear strain tensor $\varepsilon_{ij} = 1/2(\partial_j u_i + \partial_i u_j)$ and its gradient $\partial_k \varepsilon_{ij}$. The monopolar stress tensor σ_{ij} and the so-called dipolar (or double) stress tensor m_{kij} are then defined as

$$\sigma_{ij} = \frac{\partial W}{\partial \varepsilon_{ij}}, \qquad m_{kij} = \frac{\partial W}{\partial (\partial_k \varepsilon_{ij})}. \tag{3}$$

The simplest possible linear form of the strain energy density with a single length-scale parameter is

$$W = \frac{1}{2} c_{ijkl} \varepsilon_{ij} \varepsilon_{kl} + \frac{1}{2} c_{ijkl} l^2 \partial_r \varepsilon_{ij} \partial_r \varepsilon_{kl}, \tag{4}$$

where l is the internal length scale parameter. Along the plane $y = \text{const.}$, i.e., for the plane with the normal unit vector defined as $\mathbf{n} = (0, \pm 1)$, the so-called total stresses t_{yx} and t_{yy} can be defined. These stresses result from the monopolar traction conditions and have a form

$$t_{yx} = \pm\left(\tau_{yx} - \partial_x m_{xyx} - \partial_y m_{yyx} - \partial_x m_{yxx}\right),$$
$$t_{yy} = \pm\left(\tau_{yy} - \partial_x m_{xyy} - \partial_y m_{yyy} - \partial_x m_{yxy}\right). \tag{5}$$

The mode I crack tip dominant displacement field $\mathbf{u}(r,\theta)$ which determines the near crack tip opening displacement is of the form

$$\mathbf{u} = l(r/l)^{3/2}\left[A_1\mathbf{U}_1(\theta;c_{ijkl}) + A_2\mathbf{U}_2(\theta;c_{ijkl})\right], \tag{6}$$

where A_1, A_2 are the amplitude factors and r, θ are polar coordinates. These constants are unspecified by the asymptotic analysis and must be determined by a complete solution of the boundary value problem. It should be noted that (6) is derived under the condition of the stress-free crack faces (Fig. 1b) contrary to the Barenblatt model in which the nonzero stress density σ'_{yy} along the crack faces is prescribed (Fig. 1a). The vectors $\mathbf{U}_1(\theta;c_{ijkl})$ and $\mathbf{U}_2(\theta;c_{ijkl})$ have a complicated form but, for an isotropic material, they can be found in [8]. Similarly to the Barenblatt solution (1) the $r^{3/2}$ variation in (6) shows a cusp-like profile of crack faces.

The modelling of the process zone is the size-depended phenomena and it requires the theory taking a material length scale l into account. This length scale enters both the constitutive and the equilibrium equations and appends the dependency of the strain energy function on the gradients of the strains as one can see in (4). The consequence of this fact is a particular role of the total stress (5) in the fracture process. Its normal component t_{yy} is depicted in Fig. 1b, where it appeares as the full-field and the asymptotic solution ahead of the crack tip having a strong singularity $\sim r^{-3/2}$. The total stress takes on negative values thus exhibiting a cohesive-traction character along the prospective fracture zone. As shown in [8], the asymptotic solution for the total stress t_{yy} derived from (6) is a good approximation of the full-field solution in a very small distance from the crack tip ($\sim 10^{-1}l$). It appreciably deviates from the full-field solution for the larger distances and quickly tends to zero. However, the full-field solution for the total stress t_{yy} takes on positive values for $x > 0.5l$ and tends asymptotically to the limit of the classical elasticity [8].

The weakness of the SGET is the identification of the material internal length scale parameter l in (4) and (6). This crucial point can be solved by three different approaches. The first one employs the fitting of displacement fields near the crew dislocation as obtained by ab-initio (AI) approaches by the analytical SGET solution, the second one compares the critical crack tip opening displacement in the SGET FE model and the AI-aided molecular statics (MS) and the third one utilizes the fitting of the ab initio calculated phonon dispersion relations by the SGET dispersion solution. All the three methods give equivalent results, i.e., they provide identical values of the material length parameter l [12, 13].

NUMERICAL RESULTS

The FE model of a center cracked nano-panel consisting of a tungsten with elastic coefficients of the cubic structure $c_{11} = 523\,\text{GPa}$, $c_{12} = 205\,\text{GPa}$ and $c_{44} = 161\,\text{GPa}$ is introduced as the numerical example to illustrate the cohesion relation at the crack tip. The scheme of the specimen is shown in Fig. 2. A mixed formulation of FE solution of the gradient elasticity 4th-order equations was used where instead of the C^1 displacement field it utilizes ordinary C^0-continuous finite elements, see [14, 15]. Except the available software [17], an original novel method for FE solution of the gradient elasticity 4th-order equations was developed in [16]. Detailed FE calculations of the cracked nano-panel subjected to mod I loading in terms of the SGET were carried out under the plane strain conditions. Only a quarter of the nanopanel under the remote loading $\sigma = 12\times 10^3$ MPa, corresponding to the moment of unstable fracture as

predicted by atomistic simulations [13], and the crack length $a_c = 5.25$ nm were employed in the analysis. The material length scale parameter assessed from the AI-SGET analyses based on the screw dislocation and the phonon dispersions was $l = 0.25$ nm [13]. A fine mesh and opening of the upper face of the crack is depicted in Fig. 3. The scaled-up detail shows the cusp like opening of the near-tip crack faces.

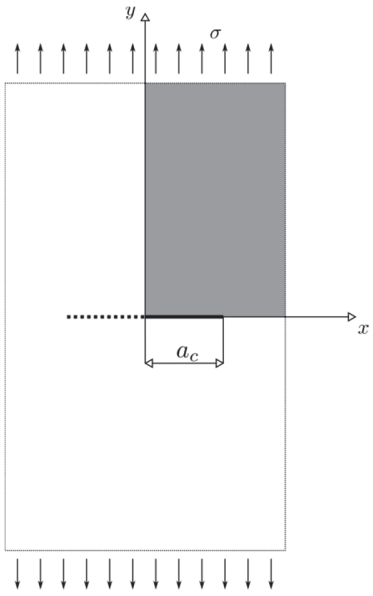

Figure 2: The dimensions of the cracked FE nano-panel and a local polar coordinate system at the crack tip.

The normal and shear strains ε_{yy} and ε_{xy}, respectively, along the crack upper face and in the near distances ahead of the crack tip $(-24l < x < 40l)$ are depicted in Fig. 4. The crack face extends along the negative axis $x < 0$. One can observe that the normal strains ε_{yy} take a finite value at the crack tip $x = 0$ contrary to the well-known classical solution, where the normal strain exhibits a square root singularity. It is also evident, that the effect of microstructure (stress gradients) is distinct only in the zone $|x| < 5l$, according to [8]. Outside this zone the normal strains ε_{yy} and ε_{xy} tend to classical ones. The shear strain ε_{xy} ahead of the crack tip $(x > 0)$ is zero due to the model symmetry and mode I loading, but it is non zero along the crack face $(x < 0)$. This is contrary to the classical linear elasticity result but in accordance with the CJP model taking the nonlinear effects near the crack tip into account [18]. One can suppose the pointwise convergence of ε_{xy} to the singular classical linear elasticity solution for the length scale parameter l tending to zero.

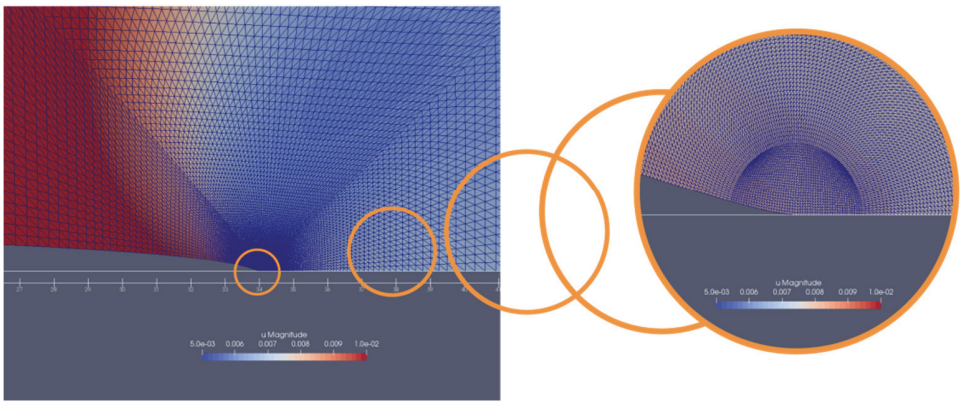

Figure 3: Upper crack face opening in SGET FE model.

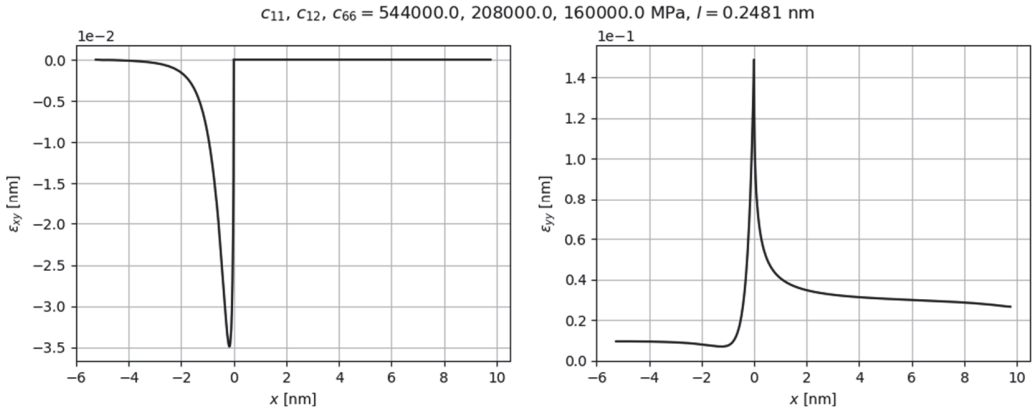

(a) (b)

Figure 4: The respective shear and normal strains ε_{xy} and ε_{yy} along the upper crack face $x < 0$ and ahead of the crack tip $x > 0$.

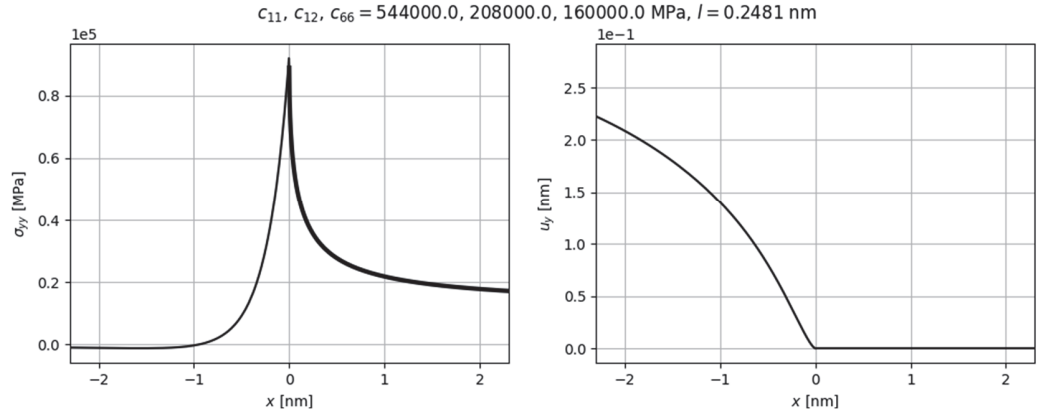

(a) (b)

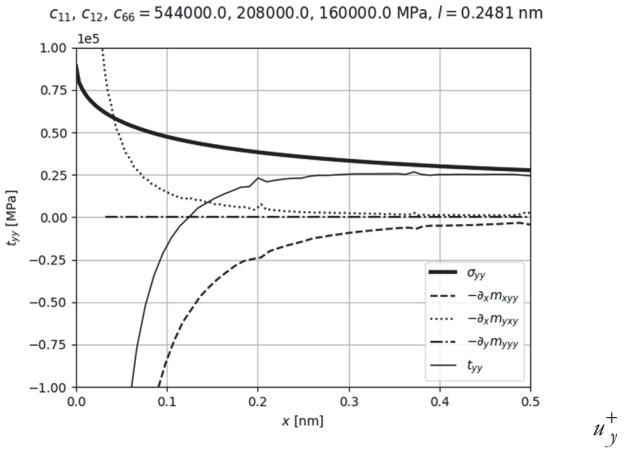

(c)

Figure 5: (a) The normal monopolar stress σ_{yy}, (b) the displacement along the upper crack face $x < 0$ and ahead of the crack tip $x > 0$, (c) the total stress t_{yy} in front of the crack tip and its components appearing in $(5)_1$. The bold part of the monopolar stress σ_{yy} in (a) corresponds to the monopolar component of the total stress t_{yy} in (c).

The distribution of the monopolar normal stress σ_{yy} along the upper crack face as well as ahead of the crack tip is also interesting from the point of view of the cohesion-decohesion relation. Fig. 5a shows the normal stress σ_{yy} with finite value at the crack tip ($x=0$) copying the distribution of the normal strain ε_{yy} from Fig. 4b. The curve of σ_{yy} for $x<0$ obeys the Barenblatt´s condition (2) and converges to the zero value and hence to the classical elasticity solution for $x<-4l$. Ahead of the crack tip ($x>0$) the convergence of σ_{yy} to the classical elasticity solution is slightly slower. The upper crack face opening is depicted in Fig. 5b, where the "closing" effect of the crack tip is obvious for $-l<x<0$. It should be emphasized that both the monopolar normal stress σ_{yy} and the displacement u_y^+ depicted in Fig. 5 well correspond to the results obtained by ab-initio adjusted molecular static codes for cracked tungsten nanoplates [13].
Contrary to the classical elasticity, the monopolar normal stress σ_{yy} is only a partial component of the total stress t_{yy}, which is responsible for the exhibiting of cohesive tractions along the crack faces. The full-filed total stress t_{yy} distribution is displayed in Fig. 5c. One can deduce the strong singular character $\sim x^{-3/2}$ of t_{yy} and a fast degreasing influence of the stress gradients for the increasing distance x from the crack tip. For $x>l$ the total stress t_{yy} tends to the classical linear elasticity monopolar stress distribution σ_{yy} ahead of the crack tip.

Conclusions

The classical linear elastic fracture mechanics, suffering from the undesirable crack-tip stress singularity, breaks down when the size of cracked components becomes less than several nanometers. The article presents a new concept of coupling methods based on atomistic and continuum mechanics approaches: The ab-initio aided strain gradient elasticity theory (AI-SGET). This method is expected to properly predict both the critical crack driving force and the critical crack tip opening displacement also for cracked nano-components. Similarly to the Barenblatt model, the SGET removes the stress singularity at the crack tip and produces a cusp-like profile of crack faces near the crack tip in accordance with atomistic models. Even the simplest form of the AI-SGET involving only one unknown material length-scale parameter l provides a reasonable form of the cohesion-decohesion stress distribution. The length-scale parameter can be determined by ab-initio methods applied to the displacement field near the screw dislocation, critical crack tip opening displacement or acoustic phonon dispersions. An important message is the fact that all these methods provide identical results. The capability of the AI-SGET method to remove the stress singularity and to exhibit a plausible near-tip cusp-like profile of crack flanks is demonstrated by the results obtained on cracked tungsten nanopanels.

Acknowledgments

The authors acknowledge a financial support of the Czech Science Foundation (the project No. 17-18566S).

References

[1] Shimada, T., Ouchi, K., Chihara, Y., Kitamura, T. (2015). Breakdown of Continuum Fracture Mechanics at the Nanoscale, Sci. Rep., 8596(5), DOI: 10.1038/srep08596.
[2] Sun, C.T., Qian, H. (2009). Brittle fracture beyond the stress intensity factor, J. Mech. Mater. Struct., 4(4), pp. 743–753, DOI: 10.2140/jomms.2009.4.743.
[3] Kotoul, M., Skalka, P. (2017). Applicability of the Critical Energy Release Rate for Predicting the Growth of a Crack in Nanoscale Materials Applying the Strain Gradient Elasticity Theory, Key Eng. Mater., 754, pp. 185–188, DOI: 10.4028/www.scientific.net/KEM.754.185.
[4] Mindlin, R.D., Eshel, N.N. (1968). On first strain-gradient theories in linear elasticity, Int. J. Solids Struct., 4(1), pp. 109–124, DOI: 10.1016/0020-7683(68)90036-X.

[5] Broberg, K.B. (1999). Crack and Fracture, Academic Press.
[6] Park, K., Paulino, G.H. (2013). Cohesive Zone Models: A Critical Review of Traction-Separation Relationships Across Fracture Surfaces, ASME. Appl. Mech. Rev., 64(6), pp. 060802-1-060802-20, DOI: 10.1115/1.4023110.
[7] Elices, M., Guinea, G.V., Gómez, J., Planas, J. (2002). The cohesive zone model: advantages, limitations and challenges, Eng. Fract. Mech., 69(2), pp. 137–163, DOI: 10.1016/S0013-7944(01)00083-2.
[8] Gourgiotis, P.A., Georgiadis, H.G. (2009). Plane-strain crack problems in microstructured solids governed by dipolar gradient elasticity, J. Mech. Phys.
[9] Aravas, N., Giannakopoulos, A.E. (2009). Plane asymptotic crack-tip solutions in gradient elasticity, Int. J. Solids Struct., 46(25–26), pp. 4478–4503, DOI: 10.1016/J.IJSOLSTR.2009.09.009.
[10] Georgiadis, H.G., Grentzelou, C.G. (2006). Energy theorems and the J-integral in dipolar gradient elasticity, Int. J. Solids Struct., 43(18–19), pp. 5690–5712, DOI: 10.1016/J.IJSOLSTR.2005.08.009.
[11] Grentzelou, C.G., Georgiadis, H.G. (2008). Balance laws and energy release rates for cracks in dipolar gradient elasticity, Int. J. Solids Struct., 45(2), pp. 551–567, DOI: 10.1016/J.IJSOLSTR.2007.08.007.
[12] Friák, M., Šesták, P., Řehák, P., Profant, T., Skalka, P., Kotoul, M. (2018). Prediction of the Critical Energy Release Rate of Nanostructured Solids Using the Laplacian Version of the Strain Gradient Elasticity Theory, Key Eng. Mater., 774, pp. 447–452, DOI: 10.4028/www.scientific.net/kem.774.447.
[13] Kotoul M., Skalka P., Profant T., Friák M., Řehák, P., Šesták, P., Černý M., Pokluda J. (2019). Prediction of the Critical Energy Release Rate of Nanostructured Solids using the Ab-initio Aided Strain Gradient Elasticity Theory (submitted for publication).
[14] Shu, J.Y., King, W.E., Fleck, N.A. (1999). Finite elements for materials with strain gradient effects, Int. J. Numer. Methods Eng., 44(3), pp. 373–91, DOI: 10.1002/(SICI)1097-0207(19990130)44:3<373::AID-NME508>3.0.CO;2-7.
[15] Phunpeng, V., Baiz, P.M. (2015). Mixed finite element formulations for strain-gradient elasticity problems using the FEniCS environment, Finite Elem. Anal. Des., 96, pp. 23–40, DOI: 10.1016/J.FINEL.2014.11.002.
[16] Skalka, P., Navrátil, P., Kotoul, M. (2016). Novel approach to FE solution of crack problems in the Laplacian-based gradient elasticity, Mech. Mater., 95, pp. 28–48, DOI: 10.1016/J.MECHMAT.2015.12.007.
[17] Alnæs, M., Blechta, J., Hake, J., Johansson, A., Kehlet, B., Logg, A., Richardson, C., Ring, J., Rognes, M.E., Wells, G.N. (2015). The FEniCS Project Version 1.5, Arch. Numer. Softw., 3(100), pp. 9–23, DOI: 10.11588/ans.2015.100.20553.
[18] James M.N., Christopher C.J., Lu Y., Patterson E.A. (2013). Local crack plasticity and its influences on the global elastic stress field. Int. J. Fatigue, 46, pp. 4-15, DOI: 10.1016/j.ijfatigue.2012.04.015.